Journal of Alloys and Compounds 671 (2016) 440–445

Contents lists available at ScienceDirect

Journal of Alloys and Compounds

journal homepage: http://www.elsevier.com/locate/jalcom

An experimental study: Role of different ambient on sulfurization of MoO_3 into MoS_2

Prabhat Kumar*, Megha Singh, Rabindar K. Sharma, G.B. Reddy

Thin Film Laboratory, Department of Physics, Indian Institute of Technology Delhi, New Delhi, 110016 India

ARTICLE INFO

Article history:
Received 7 November 2015
Received in revised form
27 January 2016
Accepted 11 February 2016
Available online 16 February 2016

Keywords:
Sulfurization
Molybdenum disulfide
Core-shell

ABSTRACT

Molybdenum disulfide (MoS_2) nanostructured thin films (NTFs) were synthesised by sulfurizing MoO_3 NTFs using three different non-conventional methods (named methods 1–3). Method 1 uses sulfur vapors, second employs H_2S/Ar gas and third adopts plasma of H_2S/Ar gas. HRTEM revealed formation of core–shell nanostructures with maximum shell thickness obtained in method 3. The samples showed uniform nanoflakes (NFs) throughout substrate, revealed by SEM, same as their precursor MoO_3. XRD and Raman analysis disclosed crystalline MoS_2 and degree of crystallinity was greatest in case of sulfurization in plasma ambient. Quantitative analysis of sulfurized films carried out by XPS shows presence of MoS_2 in all three methods with percentage found to be 18%, 87% and ~100% respectively. The effect of sulfurizing ambient on its efficiency to convert MoO_3 into MoS_2 has been studied and it was found out that plasma ambient has resulted in high quality of MoS_2 NTFs based on parameters as crystallinity, purity, uniformity and stoichiometry control.

1. Introduction

Molybdenum disulfide has become a fascinating material to study, because it is similar to graphene in terms of properties, but not nearly as difficult to synthesize. In recent years MoS_2 has attracted many researchers and scientists and motivated them to work in order to impart desirable physical and chemical properties [1]. These properties makes it a good candidate for a wide range of applications such as energy conversion [2] and storage [3], hydrogen evolution reaction [4], stretchable electronics [5], catalysts [6], and ultra-fast photonics [7]. Several methods have been reported for the synthesis of MoS_2 nanostructures, for example using mechanical exfoliation, Li et al. [8] prepared MoS_2 and WSe_2 nanosheets. Similarly solvent based exfoliation method also known as Coleman method [9] was used to obtain MoS_2 from exfoliating suspended MoS_2 flakes in organic solvent. But this way of obtaining MoS_2 have its drawbacks such as poor control over thickness and limited size. Control over thickness can be overcome by using laser [10] but the development of chemical and vapour phase growth has significant steps in obtaining good quality of MoS_2 nanostructures in term of crystallinity. Mdleleni et al. [11] reported nanostructured MoS_2 using sonochemical method. Feldman et al. [12] reported gas-phase growth of MoS_2 nested inorganic fullerenes and nanotubes. Atmospheric pressure chemical vapour deposition route was used by Lin et al. [13] to produce MoS_2 and WS_2 fullerene-like nanostructures and nano-flowers. Following chemical method a uniform and stratified MoS_2 film may not be synthesized, thereby restricting it for large scale production [1]. Additionally, these methods are susceptible to contaminations due to impurities present in chemicals used for synthesis. Films grown by chemical methods more often than not turn out to be non-uniform. In order to address these issues, like non uniformity, purity, size limitations, lack of control over final product, crystallinity, etc., sulfurization of Mo and Mo based oxide is gaining importance [14]. In this work we have carried out the sulfurization of uniformly deposited α-MoO_3 nanoflakes using three different methods. In first method, sulfurization of MoO_3 is carried out in ambient of sulfur vapors produced by evaporation of sulfur powder. In second method, sulfurization is accomplished in H_2S/Ar gas ambient, and in third method, sulfurization is achieved by treating MoO_3 in plasma of H_2S/Ar gas. A comparative study of films sulfurized using these three methods has been done, in order to figure out best suited out of these methods which not only eliminate disadvantages of other methods but also produce good quality of MoS_2. Films are studied to determine uniformity (determined by SEM), purity (examined by XPS and XRD), crystallinity (investigated by XRD and Raman), stoichiometry (analysed by XPS) and control over size of final product (probed by HRTEM). Final conclusions are drawn to comment on

* Corresponding author.
E-mail address: prabhat89k@gmail.com (P. Kumar).

http://dx.doi.org/10.1016/j.jallcom.2016.02.097
0925-8388/

quality of sulfurization derived from results obtained by above stated characterization techniques.

2. Experimental

MoO_3 nanoflakes are deposited over glass substrate using plasma assisted sublimation process (PASP) [15]. These as-deposited MoO_3 films are then sulfurized using three different methods, stated as follows. Fig. 1(A) shows experimental setup for method 1, which consists of two temperatures zones: Low temperature zone (100–300 °C) and high temperature zone (400–600 °C). Temperatures are read using a thermocouple each for different zone. Sulfur powder is kept in low temperature zone (zone 1) whereas MoO_3 NSTs is kept in high temperature zone (zone 2). Argon gas is used as carrier gas to facilitate transport of sulfur vapors from zone 1 to zone 2. Gas flow rate is kept constant at 200 sccm. Sulfur powder is heated at 150 °C in zone 1. Sulfur melts and vapors are generated which are transported to zone 2 (kept at 550 °C). Sulfur vapors reacts with MoO_3 NSTs to form MoS_2 (sample R2). Fig. 1(B) shows experimental setup for methods 2 (Sample R3) and 3 (Sample R4). It comprises of molybdenum metal strip attached with a heating assembly to supply required amount of heat for sulfurization. Sample (MoO_3 over glass substrate) is placed directly on Mo strip, which is supplied controlled current via external 10 A power supply. A thermocouple is placed near substrate to read the temperature of substrate.

Plasma assembly consists of aluminium electrodes kept at a spatial separation of 7.5 cm. Method 2 focusses on sulfurization of MoO_3 NSTs in presence H_2S/Ar gas, whereas method 3 focusses on sulfurization in presence of H_2S/Ar plasma. Partial pressure inside the vacuum chamber is maintained at 6.5×10^{-1} Torr in both the cases (methods 2 and 3). Substrate temperature is maintained at 550 °C. A mixture of H_2S/Ar gas in 1:9 ratio is supplied into vacuum chamber. Plasma is generated in case of Method 3 by applying 1000 V between electrodes. The duration of sulfurization process is 60 min for all three samples. The samples are allowed to cool down in Ar environment.

The surface microstructures of all films are studied with scanning electron microscope (ZEISS EVO Series scanning electron microscope model EVO-18). Structural analysis of films are studied

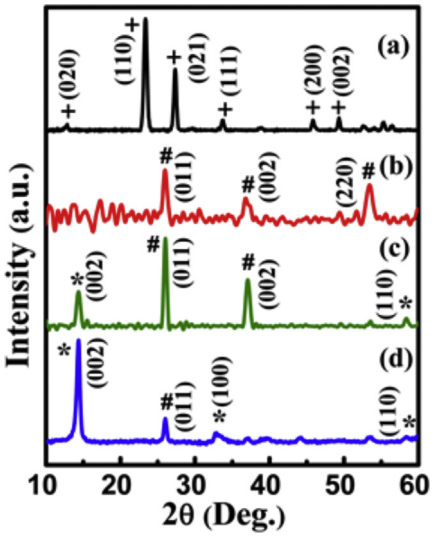

Fig. 2. X-ray diffractogram of (a) as deposited MoO_3 film and films sulfurized in: (b) Sulfur vapors ambient, (c) H_2S/Ar gas ambient and (d) H_2S/Ar plasma ambient.

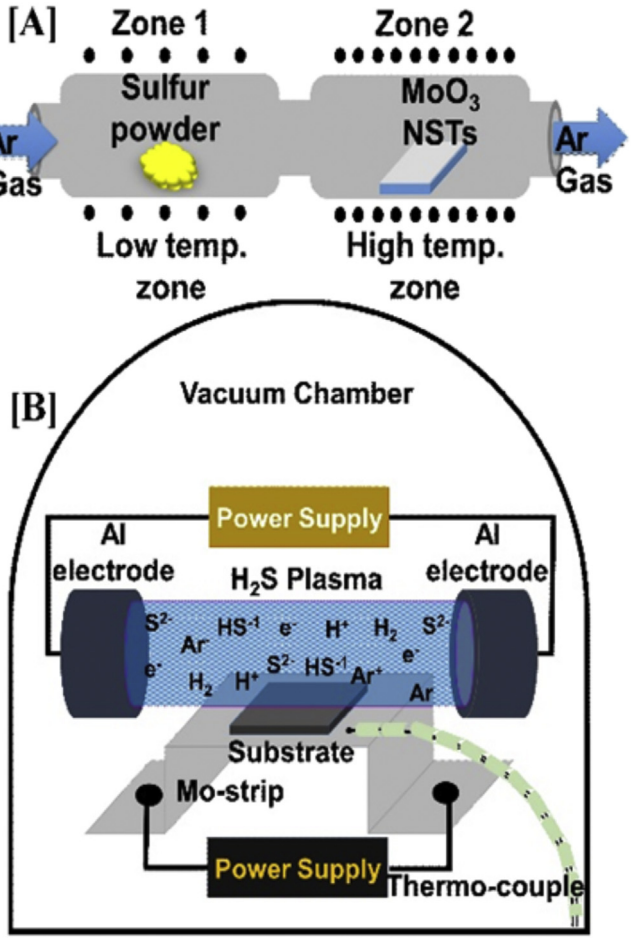

Fig. 1. Experimental set-up: (A) using sulfur powder; (B) Using H_2S/Ar gas with and without plasma.

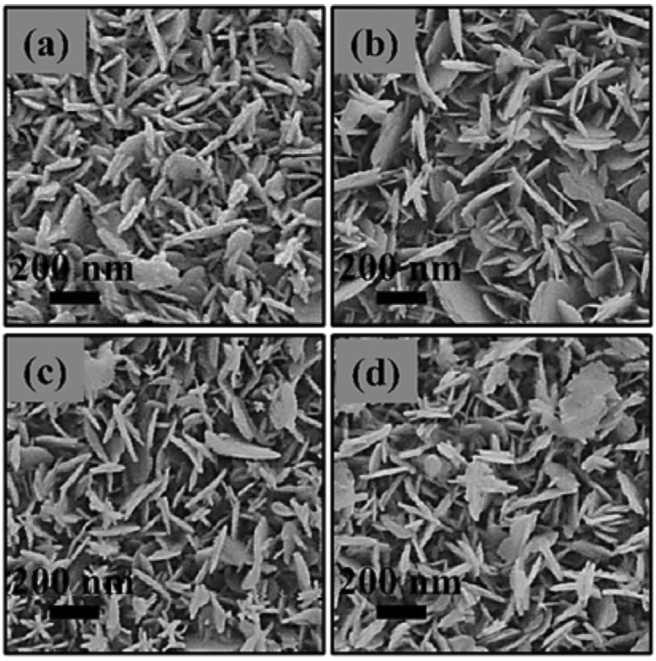

Fig. 3. SEM micrographs of (a) as deposited MoO_3 film and films sulfurized in: (b) Sulfur ambient, (c) H_2S/Ar gas ambient and (d) H_2S/Ar plasma ambient.

using Rigaku Ultima IV model X-ray diffractometer equipped with Cu-Kα radiation (λ ~ 1.54 Å) with the glancing angle kept constant at 1°. All the diffractograms are recorded in 2θ range of 10–60°, by using X-rays generated by electron beam current of 40 mA and accelerating voltage 45 kV. To study the vibrational properties of NSTs, Raman spectroscopy of Horiba Lab RAM HR Evolution (excited at 514 nm) spectroscopy are employed in the spectral range from 200 to 1000 cm^{-1}, with the resolution limit of 1 cm^{-1}. For the dimensional and the structural analysis, (TEM) micrographs of NFs are recorded using Tecnai F30 operated at 200 kV with selected area electron diffraction (SAED) pattern. X-ray photoelectron spectroscopic (XPS) studies are performed using SPECS spectrometer, with anode Mg/Al X-ray source of power 100 Watts with the resolution of 0.2 eV. The radiation used in XPS in study is Mg-K_α source.

3. Results and discussion

X-ray diffraction pattern of MoO_3 nanostructured thin film deposited on glass substrate is shown in Fig. 2(a). All the diffraction peaks recorded are distinctly assigned as an orthorhombic phase of molybdenum oxide i.e. α-MoO_3 (marked by +) and are well matched with the reported data (JCPDS card no. 89–5108, a = 3.962 Å, b = 13.858 Å and c = 3.697 Å). Fig. 2(b) shows the MoO_3 film sulfurized using method 1. In sample R2 all the peaks associated with MoO_3 have disappeared, whereas the peaks corresponding to monoclinic phase of MoO_2 (marked by #) have appeared at 2θ values of 26.11°, 37.31° and 53.34° associated to (011), (002) and (220) crystal planes respectively (JCPDS card no. 78–1073). This implies that sulfur vapors ambient caused the reduction of MoO_3 to form MoO_2. It can be noted that XRD pattern of R2 shows a higher degree of disorder as compared to MoO_3, indicating that films have poor crystallinity while precursor MoO_3 has good crystallinity. No peak related to the MoS_2 is detected in sample R2 due to lack of crystallinity and order, which is further confirmed by HRTEM analysis (discussed in later section). When the sulfurization of MoO_3 NTFs is carried out in H_2S/Ar gas, MoS_2 (marked by *; JCPDS card no. 37–1490) peak at 2θ value 14.32° is detected along with MoO_2 peaks. In this case the intensity of peak related to MoS_2 (002) plane is lesser as compared to that of (011) plane of MoO_2, showing that MoO_2 is prominent material present in sample R3. On examining further, the XRD pattern of R3, improved crystallinity is observed as peaks become sharp and more defined as compared to R2.

Fig. 2(d) shows the XRD pattern of MoO_3 NTF, sulfurized in H_2S/Ar plasma ambient (method 3). The recorded peaks correspond to MoS_2 hexagonal phase at 2θ values 14.32°, 33.12° and 58.61° associated with (002), (100) and (110) crystal planes respectively along with MoO_2 monoclinic phase peaks at 2θ value 26.11°. The peak intensity of (002) crystal plane of MoS_2 is more as compared

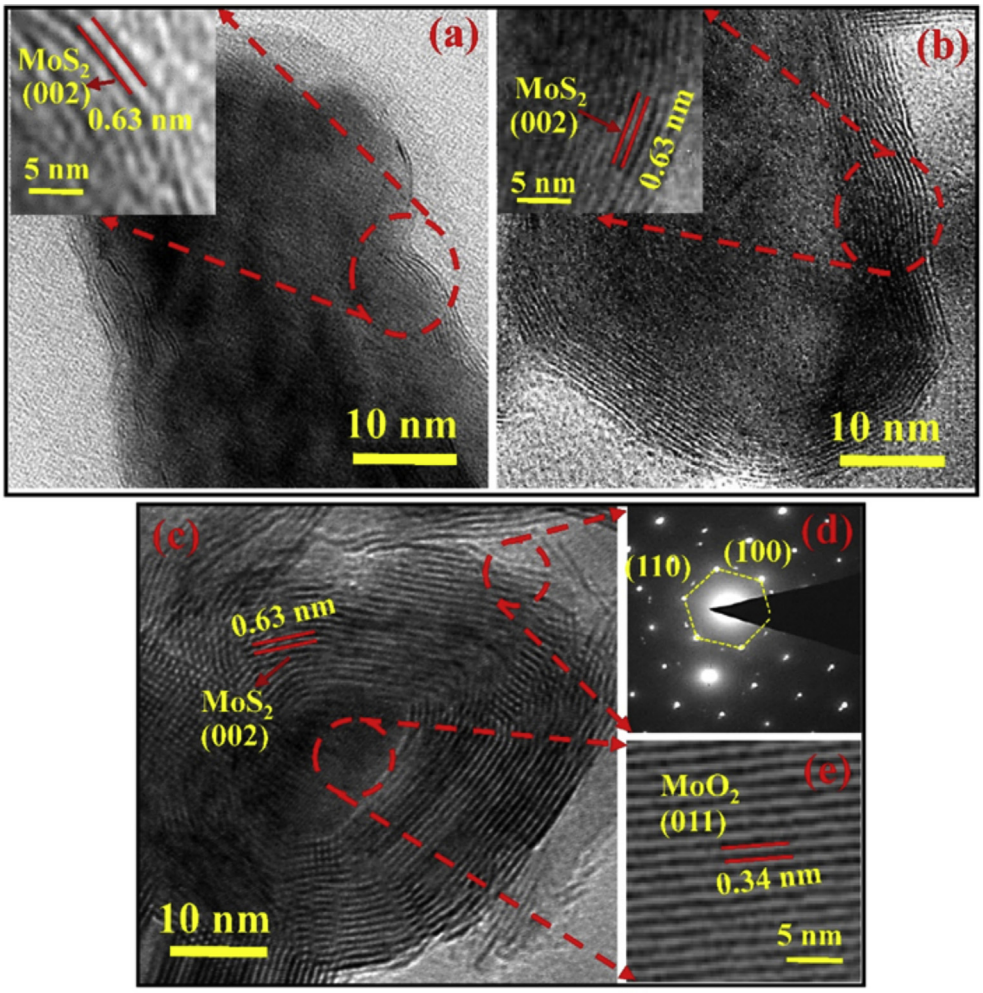

Fig. 4. HRTEM of sulfurized MoO_3 film in: (a) Sulfur vapors, (b) H_2S/Ar gases; and (c) H_2S/Ar plasma, (d) SAED pattern from the encircled region; and high resolution image recorded from the centre of nanoflakes as marked in (e).

to the intensity of MoO_2 peak of (011) crystal plane, indicating sample R4 consists mostly of MoS_2 with MoO_2 present in minor amount. The crystallinity in R4 is highest in comparison to R2 and R3. Also is observed that the degree of disorder is minimum. The XRD investigation of all sample revealed the presence of molybdenum dioxide and disulfides only. No other element or compound is present in sulfurized films, indicating films have high purity. Presence of MoO_2 is explained as a result of reduction caused by reducing agents like S in method 1, H_2S in method 2 and H, S ionic species in method 3. Since the presence of MoO_2 is most prominent in R2 and least in R4 also vice-versa for MoS_2. Therefore, it can be stated that in presence of plasma, the degree of sulfurization for conversion MoO_3 film into MoS_2 is maximum as the intensity of MoS_2 peaks get strengthen, making this method most suited method for sulfurization of MoO_3 among other studied.

In order to study the morphology of MoO_3 films sulfurized in three different media, micrographs using SEM are recorded. Fig. 3(a) shows SEM micrograph of as deposited MoO_3 NTFs. The average width and thickness of nanoflakes range from 100 to 400 nm. All the nanoflakes are vertically aligned and have stratified features. Fig. 3(b–d) shows surface morphologies of samples R2, R3 and R4 respectively sulfurized in different sulfurization environments (methods 1–3). SEM micrograph shows no noticeable difference in the surface morphology of films after sulfurization. This shows no growth has taken place on the surface of MoO_3 nanoflakes while analysing this result in conjunction with that obtained from XRD, it is therefore inferred that MoO_3 has been converted to MoS_2 and MoO_2.

To study the effect of sulfur species present in different media (i.e. sulfur vapors, H_2S gas and H_2S plasma) on surface of MoO_3 NFs at atomic level, HRTEM micrographs of samples R2, R3 and R4 are recorded, as shown in Fig. 4(a–e). The images displays MoO_2/MoS_2 core–shell nanostructures were obtained in all three methods. The only difference is thickness of MoS_2 shell, which is a parameter used for comparing the quality of films by control of size in all three methods. In the inset of Fig. 4(a) shows the HRTEM images from the outer surface of NF sulfurized in sulfur vapors, exhibited 3–4 monolayers of MoS_2 with interplanar distance of 0.63 nm. This recorded d-spacing is in good agreement with the reported d-spacing of (002) crystal plane of MoS_2 [16]. From, HRTEM image of sample R2, we can also observe that the MoS_2 is non-uniform around the nanoflake and the inset of Fig. 4 (a) shows that the MoS_2 monolayers are not neatly stacked together. Hence these two reasons can be attributed to the absence of MoS_2 peak in XRD. The possible chemical reactions in first method is given by equations (1) and (2). In method 1 (S-vapors) the conversion rate of MoO_3 into MoS_2 is low due to the presence of very less reactive sulfur species. As sulfur evaporates to form S_2 (dimer) and S_8 (oligomer) [17]. In order to generate reactive elemental sulfur species, much higher temperature is required. Normally at low temperature (~550 °C in present case) sulfur powder sublimes in form of S_2 and S_8, so create a less reactive sulfurization environment as compared to elemental S environment. But, when the sulfurization process is carried out in H_2S gas (sample R3) instead of sulfur vapors, the number of MoS_2 monolayers gets increased upto 13–16 monolayers, as shown in Fig. 4 (b). In this case the possible sulfurization reactions are given in equations (3) and (4). In method 3, H_2S/Ar plasma is chosen to sulfurize MoO_3 film. It is well reported that more than 90% species in plasma are present in the form of reactive ions so, it can be anticipated that H_2S plasma will provide more reactive sulfurization ambience. Fig. 4 (c) shows the HRTEM image of sulfurized MoO_3 film in presence of H_2S plasma. From image it is clear that number of monolayers of MoS_2 gets increased upto 25–28 in presence of plasma, which indicates that the presence of plasma not only enhanced sulfurization but also furnish the uniform sulfurization on entire MoO_3 nanoflake. Equations (5) and (6) show the.

possible reaction of MoO_3 sulfurization in H_2S/Ar plasma ambience.

$$MoO_3 + \frac{1}{2}S \rightarrow MoO_2 + \frac{1}{2}SO_2 \quad (1)$$

$$MoO_2 + 3S \rightarrow MoS_2 + SO_2 \quad (2)$$

$$MoO_3 + H_2S \rightarrow MoO_2 + H_2O + S \quad (3)$$

$$MoO_2 + H_2S \rightarrow MoS_2 + 2H_2O \quad (4)$$

$$MoO_3 + 2H^+ + 2e^- \rightarrow MoO_2 + H_2O \quad (5)$$

$$MoO_2 + 2S^* \rightarrow MoS_2 \quad (6)$$

The recorded HRTEM image from the core of nanoflake shows the d-spacing between atomic layers is 0.34 nm, which corresponds to the (011) crystal plane of monoclinic phase of MoO_2 [16] and supports the XRD results. This substantial increment in sulfurization in presence of H_2S plasma is mainly owing to the presence of large number of reactive ionic species of hydrogen (H^*, H^+) and sulfur (S^*, HS^{-1}, S^{2-}) [18], having higher reduction potential compared to the H_2S gas. Following method 3, uniform sulfurized MoO_2/MoS_2 core–shell nanostructures were obtained which had maximum monolayers in comparison to methods 1 and 2.

In order to study the process taking place at structural level Raman spectroscopy is carried out for all the samples. Fig. 5(a)

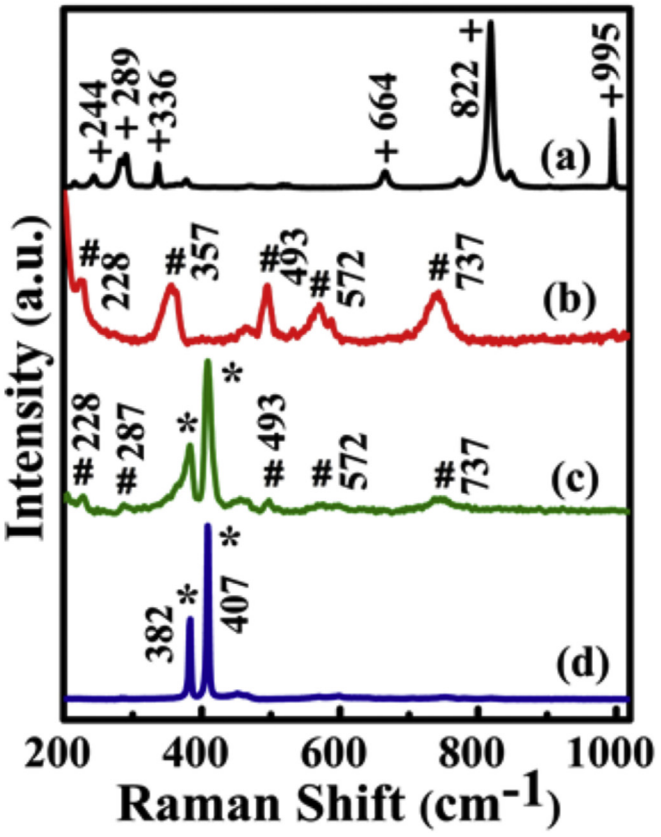

Fig. 5. Raman spectra of (a) as deposited MoO_3 film and films sulfurized in: (b) Sulfur ambient, (c) H_2S/Ar gas ambient and (d) H_2S/Ar plasma ambient.

shows the Raman spectrum of MoO_3 NTFs, with peaks present at 244, 289, 336, 664, 822 and 995 cm^{-1}. All peaks are in good agreement with those reported for α-MoO_3 [19,20]. The sharp and intense peaks evidence the presence of good crystallinity in MoO_3 film. The Raman spectrum of sample R2 is shown in Fig. 5(b), no peaks related to α-MoO_3 are detected, confirming that surface of NFs is completely reduced into MoO_2 because all the peaks observed at 228, 357, 493, 572, 737 cm^{-1} are unambiguously matched with monoclinic phase of MoO_2 [21]. However these peaks are not sharp, but broad, indicating lack of crystallinity (as confirmed in XRD of sample R2) and no peaks related to MoS_2 can be seen clearly. In Raman (Fig. 5(b)) the absence of MoS_2 peaks can be attributed to lack of crystallinity in MoS_2 and absence of perfect stoichiometry (as observed from XPS Fig. 6). Although MoS_2 is present in sample as seen in Fig. 4(a), which is also further supported by XPS analysis (discussed in later section) depicting non-stoichiometric Mo_xS_y leading to absence of MoS_2 peaks. When the sulfurization is carried out in presence of H_2S/Ar gas, two Raman peaks at 382 and 407 cm^{-1} corresponds to MoS_2 hexagonal phase [22] are observed along with peaks associated with the monoclinic MoO_2. Therefore, it can be stated that there is an increase in the rate of sulfurization as the surface of MoO_3 NTFs has been completely transformed to MoO_2 and MoS_2.

In sample R3, peaks of MoS_2 present at 382 and 407 cm^{-1} become broader which may be owing to two possible factor. First due to less crystallinity of MoS_2 and secondly due to the presence of MoO_2 monoclinic phase whose peak at 357 cm^{-1} also overlaps with the peak of MoS_2. It is worth noted that on sulfurization of MoO_3 NTFs in H_2S/Ar plasma, peaks related to only MoS_2 phase are recorded. In this case relatively sharp and more intense peaks depicting the increment in the sulfurization to form MoS_2 hexagonal phase. Hence, the Raman results supports the XRD outcomes and further confirms that maximum sulfurization is obtained only in presence of H_2S/Ar plasma, as highly crystalline films were obtained.

X-ray photoelectron spectra of MoO_3 NTF and the films sulfurized in different media are shown in Fig. 6. All peaks are calibrated with C (1s) peak which recorded at constant binding energy of 284.6 ± 0.2 eV in all samples. The XPS spectra of MoO_3 film has a Mo (3d) doublet corresponding to Mo ($3d_{5/2}$) at binding energy of 232.43 eV and Mo ($3d_{3/2}$) at binding energy of 235.49 eV with a splitting of 3.06 eV as shown in Fig. 6(D), which is the characteristic for molybdenum in a 6 + oxidation states [23]. On sulfurization of MoO_3 film in sulfur vapors, peaks corresponds to Mo (3d) are not only shifted but also get broadened as shown in Fig. 6(A). The spectrum contains three component of molybdenum, first MoO_3 at 232.43 eV (6 + oxidation state), second MoO_2 at 229.62 (4 + oxidation state), and last one MoS_2 at 228.87 eV (4 + oxidation state). The peaks corresponding to MoS_2 and MoO_2 appears at 228.87 eV and 229.62 eV respectively which makes it difficult to calculate the relative percentage of both the contents. In general to find out the relative percentage of both the components there are two methodologies [24]. First by the S/Mo ratio from wide scan using standard value of MoS_2 = 2, and second method by deconvoluting the peaks. The calculated relative percentage of MoS_2 in sample R2 is ~18% by both methods. It implies that film surface gets partially reduced to MoO_2 and MoS_2 as confirmed previously by Raman analysis.

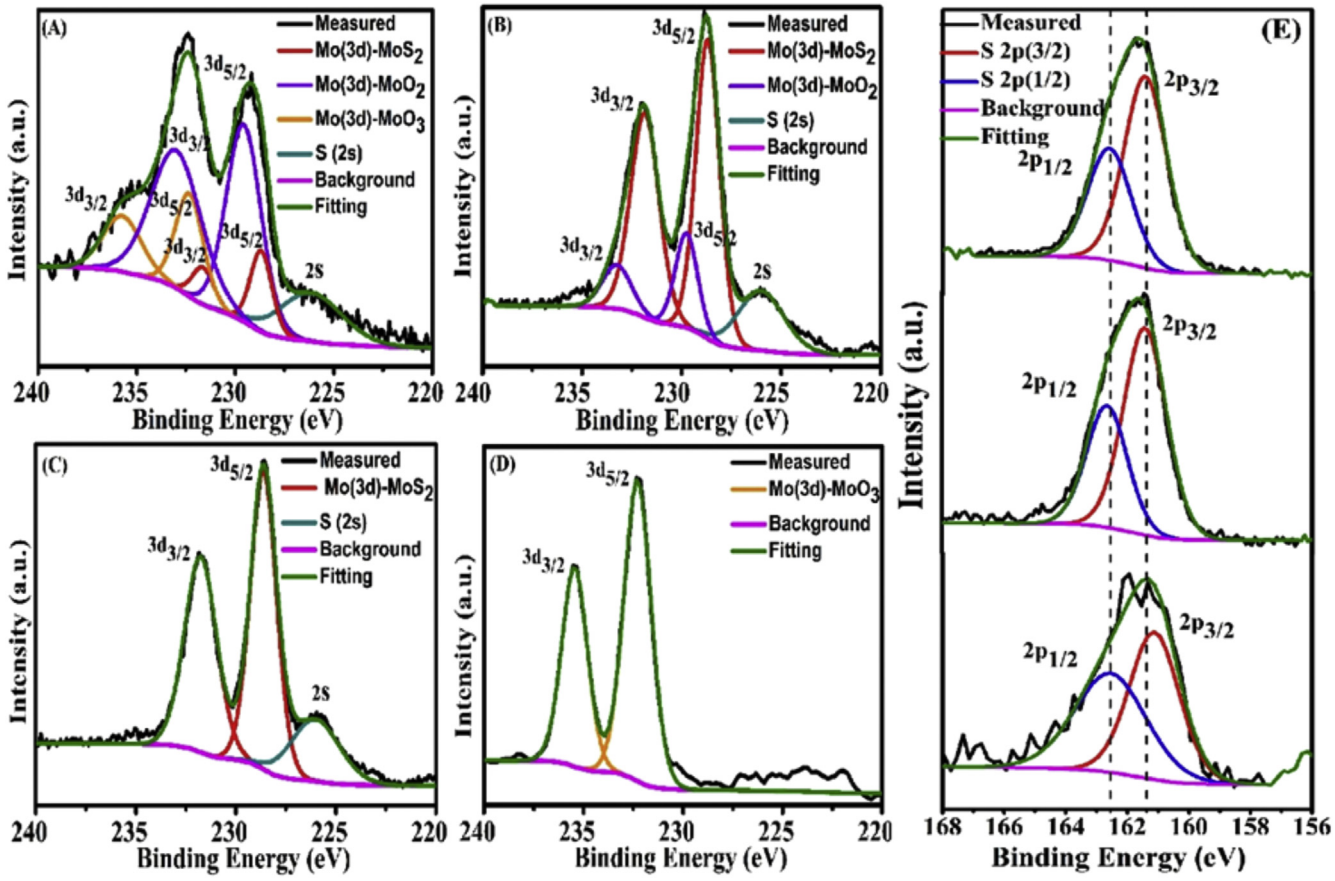

Fig. 6. XPS core level spectrum Mo of as deposited MoO_3 film (D) and films sulfurized: in Sulfur ambient (A), in H_2S/Ar gas ambient (B) and in H_2S/Ar plasma ambient (C) and core level spectrum of sulfur 2p (E).

Fig. 6(B) shows the XPS spectrum of sample R3, the percentage of MoS_2 has increased as compared to the sample R2, the calculated relative percentages of MoS_2 and MoO_2 are 87% and 13% respectively. Absence of MoO_3 peak depicts that film surface has been completely reduced and sulfurized to form MoO_2 and MoS_2. As H_2S/Ar gas is replaced by its plasma under the same experimental conditions, complete conversion of MoO_3 film surface into MoS_2 is obtained (~100%). It implies that in plasma, reactive species of sulfur (S^*, S^{2-} and HS^{-1}) and hydrogen (H^+) provide higher of sulfurization rate as compared to H_2S gas and sulfur powder. The spectrum of sulfur component is shown in Fig. 6(E). It shows a doublet of S ($2P_{3/2}$) at 161.5 eV and S ($2P_{1/2}$) at 162.9 eV [25]. Examination of S (2p) peak shows that sulfur is present in S^{2-} oxidation state, confirming the formation of MoS_2. The sulfur peak in sample R2 is much broader as compared to the peaks obtained in other two cases. This may be due to the presence of thiomolybdates species [24], these structures have core of MoxSy, ($x \neq y \neq 1$) with the binding energy in the range of 162.3–163.5 eV. These species formation is related to anion vacancies in MoS_2 lattice where S/Mo ratio is near unity. Another reason for broadening, may be due to non-stoichiometric ratio of Mo and S. In case of sample R3 and R4 the presence of sharp sulfur peaks confirms the improvement in crystalline nature of film. Therefore, XPS results shows, method 3 has displayed highest percentage of MoS_2, thus can be adopted for synthesis of MoS_2 nanostructures.

4. Conclusions

In summary, sulfurization of MoO_3 nanostructured thin film has been carried out using three different sulfurizing environments and resultant films have been studied in order to determine the method best suited based on crystallinity, purity, uniformity, stoichiometry and size control. The three sulfurization environments are sulfur vapours (method 1), H_2S/Ar gas (method 2) and H_2S/Ar gas plasma (method 3). Structural analysis shows that all the films have been transformed to monoclinic MoO_2 and hexagonal MoS_2 phase. Maximum sulfurization is accomplished in plasma environment, as highly crystalline film after sulfurization were obtained, which is further confirmed by the HRTEM results. Also HRTEM result revealed that MoO_3 nanoflake has acquired core–shell structure after sulfurization with maximum thickness of MoS_2 is obtained (~16 nm) in case of plasma. XPS analysis shows that three components of Mo was present in method 1, whereas in method 2, MoS_2 was found along with MoO_2. But in third method of sulfurization the surface is completely sulfurized to form MoS_2 with stoichiometric ratio of Mo and sulfur (~2). Hence, by comparing these three methods, plasma assisted sulfurization (method 3) yielded best quality MoS_2 nanostructured thin film. This approach of using plasma for sulfurization of MoO_3 nanostructures paves the large scale route to synthesize MoS_2 nanostructures, by varying different growth parameters, therefore making this approach tuneable pliable for obtaining sulfurized films.

Acknowledgement

We thankfully acknowledge the use of Ultima IV Rigaku X-ray Diffractometer, Raman spectrometer in NRF and XPS facility (partially funded by FIST grant of DST) at I.I.T. Delhi.

References

[1] I. Song, C. Park, H.C. Choi, Synthesis and properties of molybdenum disulphide: from bulk to atomic layers, RSC Adv. 5 (2015) 7495–7514, http://dx.doi.org/10.1039/C4RA11852A.

[2] S. Wi, H. Kim, M. Chen, H. Nam, L.J. Guo, E. Meyhofer, et al., Enhancement of photovoltaic response in multilayer MoS_2 induced by plasma doping, ACS Nano 8 (2014) 5270–5281, http://dx.doi.org/10.1021/nn5013429.

[3] S. Ding, D. Zhang, J.S. Chen, X.W. (David) Lou, Facile synthesis of hierarchical MoS_2 microspheres composed of few-layered nanosheets and their lithium storage properties, Nanoscale 4 (2012) 95–98, http://dx.doi.org/10.1039/C1NR11552A.

[4] Z. Chen, D. Cummins, B.N. Reinecke, E. Clark, M.K. Sunkara, T.F. Jaramillo, Core-shell MoO_3-MoS_2 nanowires for hydrogen evolution: A functional design for electrocatalytic materials, Nano Lett. 11 (2011) 4168–4175, http://dx.doi.org/10.1021/nl2020476.

[5] W. Wu, L. Wang, Y. Li, F. Zhang, L. Lin, S. Niu, et al., Piezoelectricity of single-atomic-layer MoS_2 for energy conversion and piezotronics, Nature 514 (2014) 470–474, http://dx.doi.org/10.1038/nature13792.

[6] G. Zhou, X. Xu, J. Yu, B. Feng, Y. Zhang, J. Hu, et al., Vertically aligned MoS_2/MoO_x heterojunction nanosheets for enhanced visible-light photocatalytic activity and photostability, Cryst. Eng. Comm. 16 (2014) 9025–9032, http://dx.doi.org/10.1039/C4CE01169D.

[7] H. Zhang, S.B. Lu, J. Zheng, J. Du, S.C. Wen, D.Y. Tang, et al., Molybdenum disulfide (MoS_2) as a broadband saturable absorber for ultra-fast photonics, Opt. Express 22 (2014) 7249, http://dx.doi.org/10.1364/OE.22.007249.

[8] H. Li, J. Wu, Z. Yin, H. Zhang, Preparation and Applications of Mechanically Exfoliated Single-Layer and Multilayer MoS_2 and WSe_2 Nanosheets, Acc. Chem. Res. 47 (2014) 1067–1075, http://dx.doi.org/10.1021/ar4002312.

[9] J.N. Coleman, M. Lotya, A. O'Neill, S.D. Bergin, P.J. King, U. Khan, et al., Two-dimensional nanosheets produced by liquid exfoliation of layered materials, Science 331 (2011) 568–571, http://dx.doi.org/10.1126/science.1194975.

[10] A. Castellanos-Gomez, M. Barkelid, A.M. Goossens, V.E. Calado, H.S.J. Van Der Zant, G.A. Steele, Laser-thinning of MoS_2: On demand generation of a single-layer semiconductor, Nano Lett. 12 (2012) 3187–3192, http://dx.doi.org/10.1021/nl301164v.

[11] M.M. Mdeleni, T. Hyeon, K.S. Suslick, Sonochemical synthesis of nanostructured molybdenum sulfide, J.Am.Chem. Soc. 120 (1998) 6189–6190, http://dx.doi.org/10.1021/ja9800333.

[12] Y. Feldman, E. Wasserman, D.J. Srolovitz, R. Tenne, High-Rate, Gas-Phase Growth of MoS_2 Nested Inorganic Fullerenes and Nanotubes, Science 267 (1995) 222–225, http://dx.doi.org/10.1126/science.267.5195.222.

[13] X.L. Li, J.P. Ge, Y.D. Li, Atmospheric pressure chemical vapor deposition: An alternative route to large-scale MoS_2 and WS_2 inorganic fullerene-like nanostructures and nanoflowers, Chem.-A Eur. J. 10 (2004) 6163–6171, http://dx.doi.org/10.1002/chem.200400451.

[14] X. Li, H. Zhu, Two-dimensional MoS2: Properties, preparation, and applications, J. Mater 1 (2015) 33–44, http://dx.doi.org/10.1016/j.jmat.2015.03.003.

[15] R.K. Sharma, G.B. Reddy, Synthesis and characterization of α -MoO_3 microspheres packed withnanoflakes, J. Phys. D. Appl. Phys.47 65305 (2014). http://stacks.iop.org/0022-3727/47/i=6/a=065305.

[16] W. Zhou, D. Hou, Y. Sang, S. Yao, J. Zhou, G. Li, et al., MoO_2 nanobelts@nitrogen self-doped MoS2 nanosheets as effective electrocatalysts for hydrogen evolution reaction, J. Mater. Chem. A 2 (2014) 11358, http://dx.doi.org/10.1039/c4ta01898b.

[17] R. Morrish, R. Silverstein, C.A. Wolden, Synthesis of stoichiometric FeS_2 through plasma-assisted sulfurization of Fe_2O_3 nanorods, J. Am. Chem. Soc. 134 (2012) 17854–17857, http://dx.doi.org/10.1021/ja307412e.

[18] G.-B. Zhao, S. John, J.-J. Zhang, J.C. Hamann, S.S. Muknahallipatna, S. Legowski, et al., Production of hydrogen and sulfur from hydrogen sulfide in a nonthermal-plasma pulsed corona discharge reactor, Chem. Eng. Sci. 62 (2007) 2216–2227, http://dx.doi.org/10.1016/j.ces.2006.12.052.

[19] R.K. Sharma, G.B. Reddy, Controlled growth of vertically aligned MoO_3 nanoflakes by plasma assisted paste sublimation process, J. Appl. Phys. 114 (2013), 184310-(1 to 7).

[20] D. Chen, M. Liu, L. Yin, T. Li, Z. Yang, X. Li, et al., Single-crystalline MoO_3 nanoplates: topochemical synthesis and enhanced ethanol-sensing performance, J. Mater. Chem. 21 (2011) 9332, http://dx.doi.org/10.1039/c1jm11447f.

[21] P.A. Spevack, N.S. Mcintyre, Thermal Reduction of MoO_3, J. Phys. Chem. C 96 (1992) 9029–9035, http://dx.doi.org/10.1021/j100201a062.

[22] B.C. Windom, W.G. Sawyer, D.W. Hahn, A raman spectroscopic study of MoS_2 and MoO_3: Applications to tribological systems, Tribol. Lett. 42 (2011) 301–310, http://dx.doi.org/10.1007/s11249-011-9774-x.

[23] A.M. de Jong, H.J. Borg, L.J. van IJzendoorn, V.G.F.M. Soudant, V.H.J. de Beer, J.A.R. van Veen, et al., Sulfidation mechanism by molybdenum catalysts supported on silica/silicon(100) model support studied by surface spectroscopy, J. Phys. Chem. 97 (1993) 6477–6483, http://dx.doi.org/10.1021/j100126a024.

[24] P.A. Spevack, N.S. McIntyre, A Raman and XPS Investigation of Supported Molybdenum Oxide Thin Films. 2. Reactions with Hydrogen Sulfide, J. Phys. Chem. 97 (1993) 11031–11036, http://dx.doi.org/10.1021/j100144a021.

[25] T. Weber, J.C. Muijsers, J.H.M.C. van Wolput, C.P.J. Verhagen, J.W. Niemantsverdriet, Basic Reaction Steps in the Sulfidation of Crystalline MoO_3 to MoS_2, As Studied by X-ray Photoelectron and Infrared Emission Spectroscopy, J. Phys. Chem. 100 (1996) 14144–14150, http://dx.doi.org/10.1021/jp961204y.